

# Probing Extra Dimensions by Invisible Higgs Decays at the LHC and a future LC

Jack Gunion

Davis Institute for High Energy Physics, U.C. Davis

Collaborators: M. Battaglia, D. Dominici, J. Wells

SUSY2004, Tsukuba, June 19, 2004

# Outline

- Theoretical Summary
- LHC and LC Discovery Potential
- Using LHC and LC data to determine model parameters
- Conclusions

# Bibliography

## References

- [1] N. Arkani-Hamed, S. Dimopoulos, and G. R. Dvali. *Phys. Lett.*, B429:263–272, 1998.
- [2] G. F. Giudice, R. Rattazzi, and J. D. Wells. *Nucl. Phys.*, B595:250–276, 2001.
- [3] J. D. Wells. hep-ph/0205328.
- [4] Atlas: Detector and physics performance; technical design report; volume 1. CERN-LHCC-99-14.
- [5] Atlas: Detector and physics performance; technical design report; volume 2. CERN-LHCC-99-15.
- [6] S. Abdullin *et al.* CMS NOTE-2003/033.

- [7] M Schumacher. Note. LC-PHSM 2003-096.
- [8] Oscar J. P. Eboli and D. Zeppenfeld. Observing an invisible higgs boson. *Phys. Lett.*, B495:147–154, 2000.
- [9] Graham W. Wilson. LC-PHSM-2001-010, Feb. 2001.

## Theoretical Issues

- The simplest model of extra dimensions is the ADD [1] model in which only gravity propagates in the extra dimensions and all the extra dimensions have the same compactification radius.

All SM particles live only on the 3-brane.

- In this model, the KK excitations (gravitensors and graviscalars) are invisible to 3-brane detectors since they propagate mainly in the bulk.

Hence, a canonical signature for ADD extra dimensions is substantial missing energy associated with various kinds of events.

- The generic signature involving  $\cancel{E}_T$  is production of a  $jets/\gamma + \cancel{E}_T$  final state, in which the KK gravitational excitations are radiated away into the extra dimension to create the  $\cancel{E}_T$ .
- However, it is also generically the case there will be a mixing (on the 3-brane) between the Higgs boson of the SM and the curvature tensor.

In ADD models, the interaction between the Higgs complex doublet field  $H$  and the Ricci scalar curvature  $R$  of the induced 4-dimensional metric  $g_{ind}$  is given by the following action

$$S = -\xi \int d^4x \sqrt{g_{ind}} R(g_{ind}) H^\dagger H . \quad (1)$$

After the usual shift  $H = (\frac{v+h}{\sqrt{2}}, 0)$ , this interaction leads to the mixing term [2]

$$\mathcal{L}_{\text{mix}} = \epsilon h \sum_{\vec{n}>0} s_{\vec{n}} \quad (2)$$

with

$$\epsilon = -\frac{2\sqrt{2}}{M_{\text{P}}} \xi v m_h^2 \sqrt{\frac{3(\delta - 1)}{\delta + 2}} . \quad (3)$$

Above,  $M_{\text{P}} = (8\pi G_N)^{-1/2}$  is the reduced Planck mass,  $\delta$  is the number of extra dimensions,  $\xi$  is a dimensionless parameter and  $s_{\vec{n}}$  is a graviscalar KK excitation with mass  $m_{\vec{n}}^2 = 4\pi^2 \vec{n}^2 / L^2$ ,  $L$  being the size of each of the extra dimensions.

- The above mixing requires re-diagonalizing to the physical eigenstates  $h'$

and  $s'_{\vec{n}}$  (which are mixtures of the SM Higgs  $h$  and the graviscalars  $s_{\vec{n}}$ ).

The  $s'_{\vec{n}}$  eigenvalues are nearly continuous and so those near in mass to the  $h'$  act coherently together with the  $h'$

- Consider the amplitude for  $I \rightarrow h' + \sum_{\vec{n}>0} s'_{\vec{n}} \rightarrow F$ , where  $I$  and  $F$  are SM particle initial and final states (such as  $I = W^*W^*$  and  $F = b\bar{b}$ ).

One finds via a very direct and brute force computation the following result:

$$\mathcal{A} = \frac{ig_{Ih}g_{Fh}}{p^2 - m_h^2 + im_h\Gamma_h^{SM} + F(p^2) + iG(p^2)}, \quad (4)$$

where

$$- \sum_{\vec{n}>0} \frac{\epsilon^2}{p^2 - m_{\vec{n}}^2 + i\epsilon'} \equiv F(p^2) + iG(p^2). \quad (5)$$

We see that the coherently summed amplitude takes the form of a SM-strength coupling structure multiplied by a modified Higgs-like propagator, where  $F(p^2)$  leads to mass and wave function renormalization for the effective Higgs propagator while  $G(p^2)$  will lead to a momentum-dependent correction to the Higgs width.

For example, we would have  $m_{h_{eff}}^2 - m_h^2 + F(m_{h_{eff}}^2) = 0$ , where  $m_{h_{eff}}$  is the pole location for the ‘effective’ coherent state  $h' + \sum_{\vec{n}>0} s'_{\vec{n}}$ . It is a kind of renormalized physical eigenstate mass.

In the narrow width approximation, as justified if both  $m_h \Gamma_h^{SM}$  and  $G(m_{h_{eff}}^2)$  are small compared to  $m_h^2$ , we see that, aside from (small) mass renormalization and wave function renormalization effects, the main effect of the mixing is to add an (invisible) width of size  $G(m_{h_{eff}}^2)/m_h$  to the SM Higgs width.

This is the approximation of [2].

- For a  $WW$  fusion initial state and a SM final state  $F$ , the result of taking  $|\mathcal{A}|^2$  and integrating over  $dp^2$  in the narrow width approximation is to yield a net cross section given by

$$\sigma(WW \rightarrow h' + \sum_{\vec{m}>0} s'_{\vec{m}} \rightarrow F) = \sigma_{SM}(WW \rightarrow h \rightarrow F) \left[ \frac{1}{1 + F'(m_{h_{eff}}^2)} \right] \times \left[ \frac{\Gamma_{h \rightarrow F}^{SM}}{\Gamma_h^{SM} + \Gamma_{h_{eff} \rightarrow graviscalar}} \right]. \quad (6)$$

Here, we have defined the invisible mixing width by  $\Gamma_{h_{eff} \rightarrow graviscalar} \sim G(m_h^2)/m_h$ , see Eq. (4), as appropriate to the extent that  $m_{h_{eff}} \sim m_h$ .

**Note the appearance of the unmixed SM cross section above.**

- For the invisible graviscalar final states,  $\sigma(WW \rightarrow h' + \sum_{\vec{n}>0} s'_{\vec{n}} \rightarrow graviscalar)$  is obtained by replacing  $\Gamma_{h \rightarrow F}^{SM}$  by  $\Gamma_{h_{eff} \rightarrow graviscalar}$  in Eq. (6) above.
- Simple estimates suggest that mass and wave function renormalization effects are small (so long as  $m_h$  is not large).
- The net result of this discussion is that the coherently summed amplitude will give the SM cross section multiplied by a branching ratio to the final state that must be computed with the inclusion of the (invisible)  $h_{eff} \rightarrow graviscalars$  width obtained above that arises from the mixing (or oscillation) of the Higgs itself into the closest KK graviscalar levels.
- We reemphasize that these graviscalars are invisible since they are weakly interacting and mainly reside in the extra dimensions whereas the Higgs resides on the brane.

The invisible mixing width,  $\Gamma_{h_{eff} \rightarrow graviscalar} \equiv G(m_h^2)/m_h$ , see Eq. (4), is given by [2, 3]

$$m_h \Gamma_{h_{eff} \rightarrow graviscalar} = -\epsilon^2 \Im \sum_{\vec{n} > 0} \frac{1}{m_h^2 - m_{\vec{n}}^2 + i\epsilon'}, \quad (7)$$

where  $\epsilon' > 0$  provides the usual pole location instruction in the complex plane.

- We evaluate this sum by converting to continuum notation in the “usual” way and obtain:

$$\begin{aligned} \Gamma_{h_{eff} \rightarrow graviscalar} &= 2\pi \xi^2 v^2 \frac{3(\delta - 1)}{\delta + 2} \frac{m_h^{1+\delta}}{M_D^{2+\delta}} S_{\delta-1} \\ &\sim (16 \text{ MeV}) 20^{2-\delta} \xi^2 S_{\delta-1} \frac{3(\delta - 1)}{\delta + 2} \left( \frac{m_h}{150 \text{ GeV}} \right)^{1+\delta} \\ &\quad \times \left( \frac{3 \text{ TeV}}{M_D} \right)^{2+\delta}. \end{aligned} \quad (8)$$

**Note:** The result (8) is a factor of 2 larger than found in Refs. [2, 3].

As we shall see,  $\Gamma_{h_{eff} \rightarrow graviscalar}$  is typically much larger than  $\Gamma_h^{SM}$  when  $m_h$  is small.

- There are additional sources of invisible decays that must be taken into account if  $m_h$  is large ( $m_h \gtrsim 500$  GeV) and  $M_D$  is close to  $m_h$ .

The most important of these is decays of  $h', s'_{\vec{n}}$  to two graviscalars. This can be a  $\lesssim 5\%$  correction when  $\delta = 2$  and  $m_h \sim M_D \gtrsim 800$  GeV if  $\xi$  is taken as large as consistent with  $\Gamma_{h_{eff} \rightarrow graviscalar} \lesssim (3 - 4) \times m_h$ . If  $\delta > 2$ , the two-graviscalar decays are negligible under this restriction.

- In what follows, our plots will at times be using the narrow width approximation in regions where  $\Gamma_{h_{eff} \rightarrow graviscalar}$  is quite large.

In such cases, our results should be regarded as a first pass on the issues we are studying.

If invisible Higgs decays are observed, one will want to use the full momentum dependent form of  $G(p^2)$  if the invisible decay width is large.

## Invisible Width and Branching Ratio Results

- Our parameters are  $M_D$ ,  $\delta$  and  $\xi$  (we assume that  $m_h$  will be well measured in some SM channel at the LHC or in  $e^+e^- \rightarrow ZX$  at a future LC).
- In the following, we plot contours of fixed  $\Gamma_{h_{eff} \rightarrow graviscalar}$  (left) and fixed  $BR(h_{eff} \rightarrow graviscalar)$  (right) in the  $M_D$  (TeV) –  $\xi$  parameter space for various  $m_h$  and  $\delta$  cases.
- In order of increasing  $\xi$  values, the width contours correspond to: 0.0001 GeV (large blue dashes), 0.001 GeV (solid red line), 0.01 GeV (green long dash – short dash line), 0.1 GeV (short cyan dashes), 1 GeV (purple dots), 10 GeV (long black dashes), 100 GeV (chartreuse long dashes with double dots), and 1000 GeV (short green solid line at high  $\xi$  and low  $M_D$ ).
- The  $BR$  contours in order of increasing  $\xi$  values correspond to: 0.0001 (large blue dashes), 0.0005 (solid red line), 0.001 (green long dash – short dash line), 0.005 (short cyan dashes), .01 (purple dots), .05 (long black

dashes), 0.1 (chartreuse long dashes with double dots), and 0.5 (green dashes), and 0.85 (red long dash, short dot line at high  $\xi$  and low  $M_D$ ).

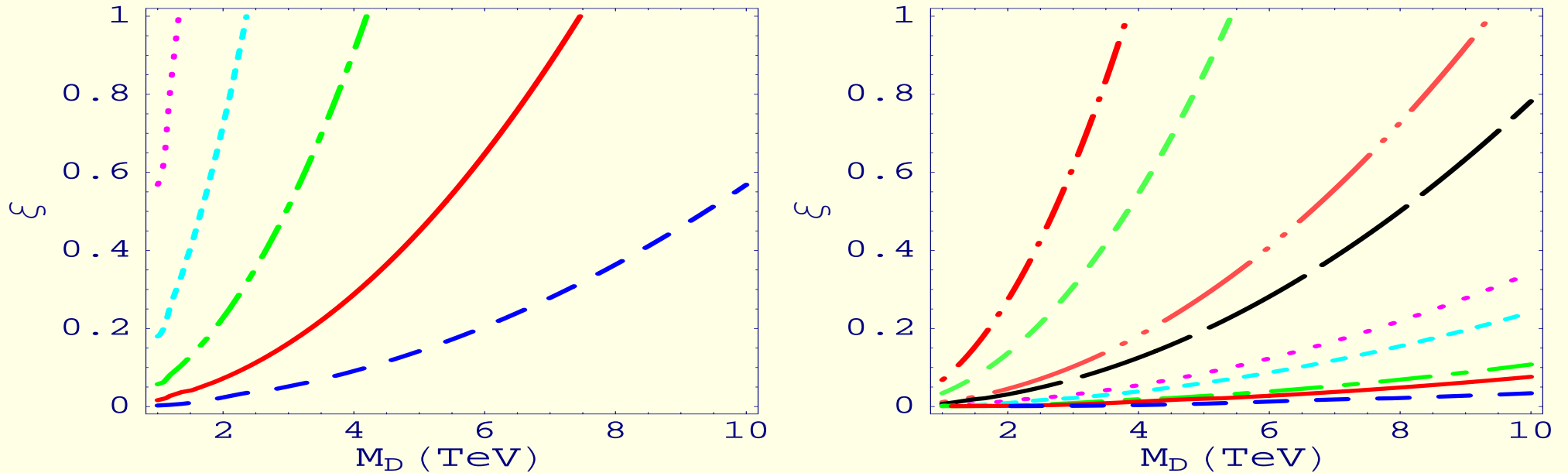


**Figure 1:**  $m_h = 120$  and  $\delta = 2$ .

Since  $\Gamma_h^{SM} \sim 3.6$  MeV for  $m_h = 120$  GeV the plotted width contours in the left-hand plots at 0.001 GeV and higher represent substantial corrections to the expected Higgs width, as apparent from the right-hand plots that show the branching ratio contours.

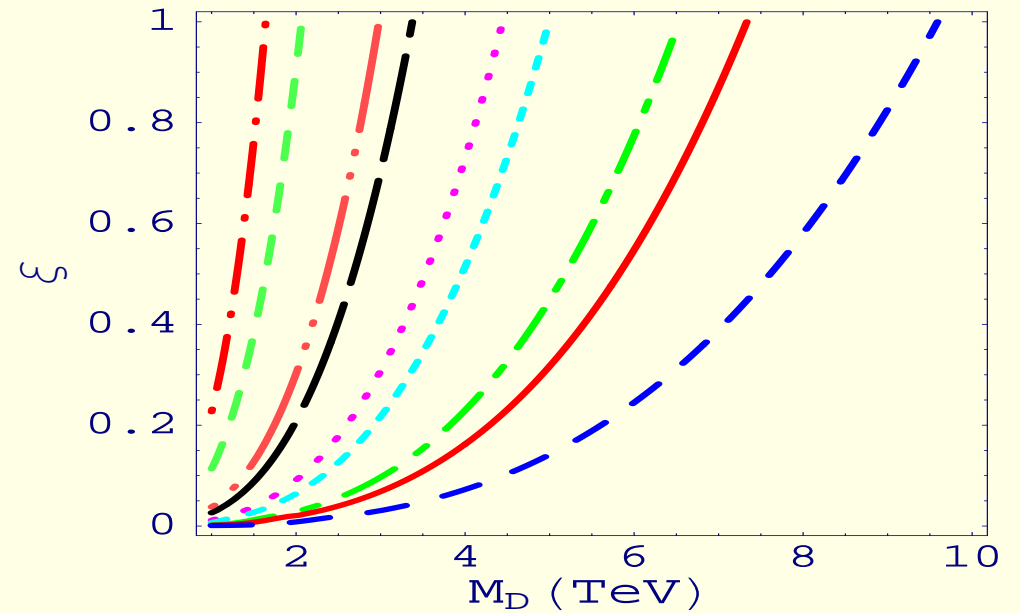
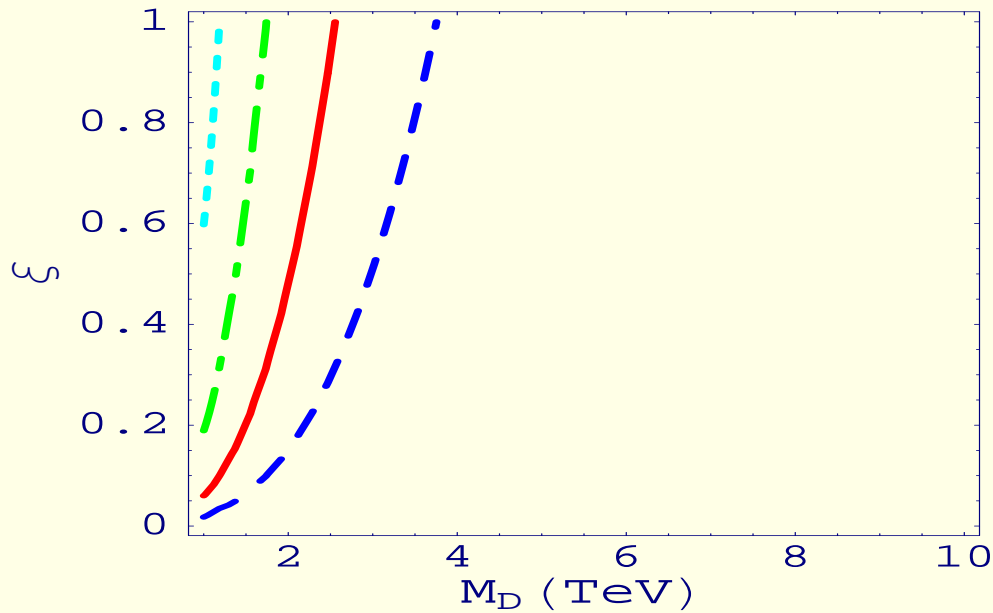


**Figure 2:**  $m_h = 120$  GeV and  $\delta = 4$ .

Larger values of  $\xi$  and smaller values of  $M_D$  are needed to get the same level of invisible width when  $\delta = 4$ .

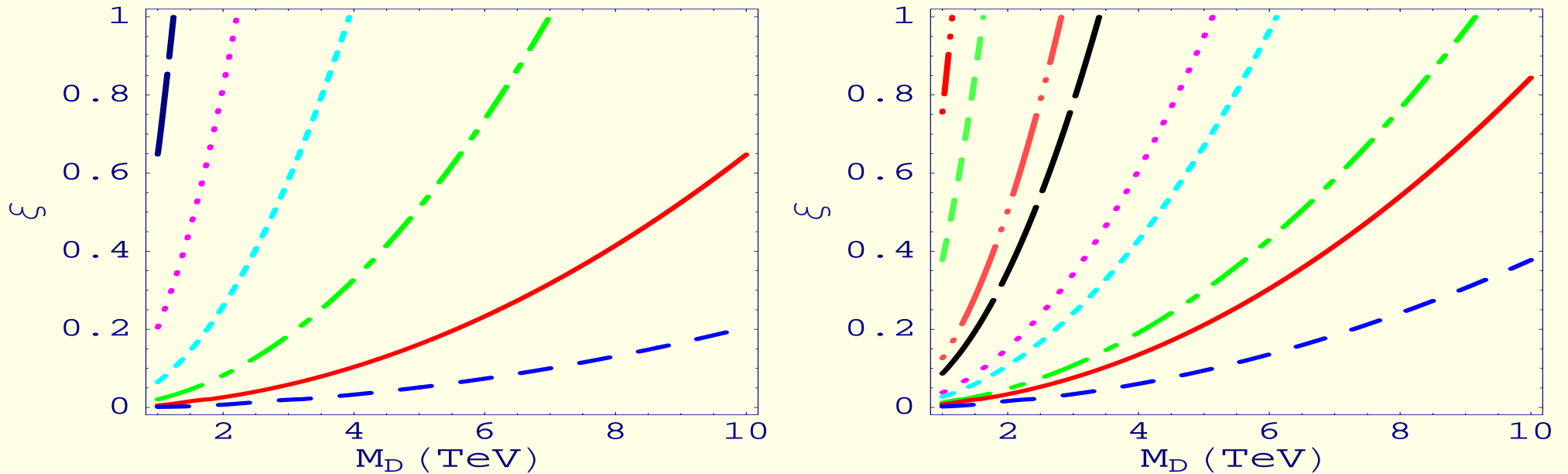
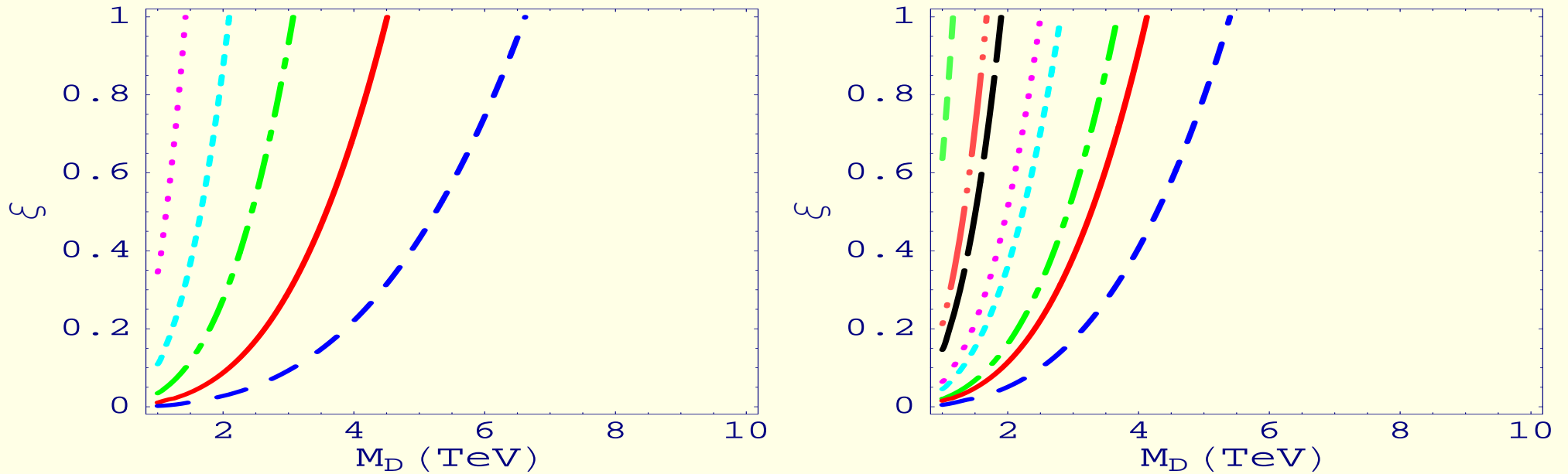


Figure 3:  $m_h = 237$  GeV and  $\delta = 2$ .

We also examine a Higgs of mass 237 GeV (the current 95% CL upper limit from LEP data with  $m_t = 178$  GeV). Above is the  $\delta = 2$  case.

Note that even though the invisible width is larger than in the  $m_h = 120$  GeV,  $\delta = 2$  case, the invisible branching ratio is smaller since  $\Gamma_h^{SM}$  is much larger in this case.



**Figure 4:**  $m_h = 237$  GeV and  $\delta = 4$ .

**Again,  $\delta = 4$  leads to smaller invisible width compared to  $\delta = 2$  at the same  $M_D$  and  $\xi$  values.**

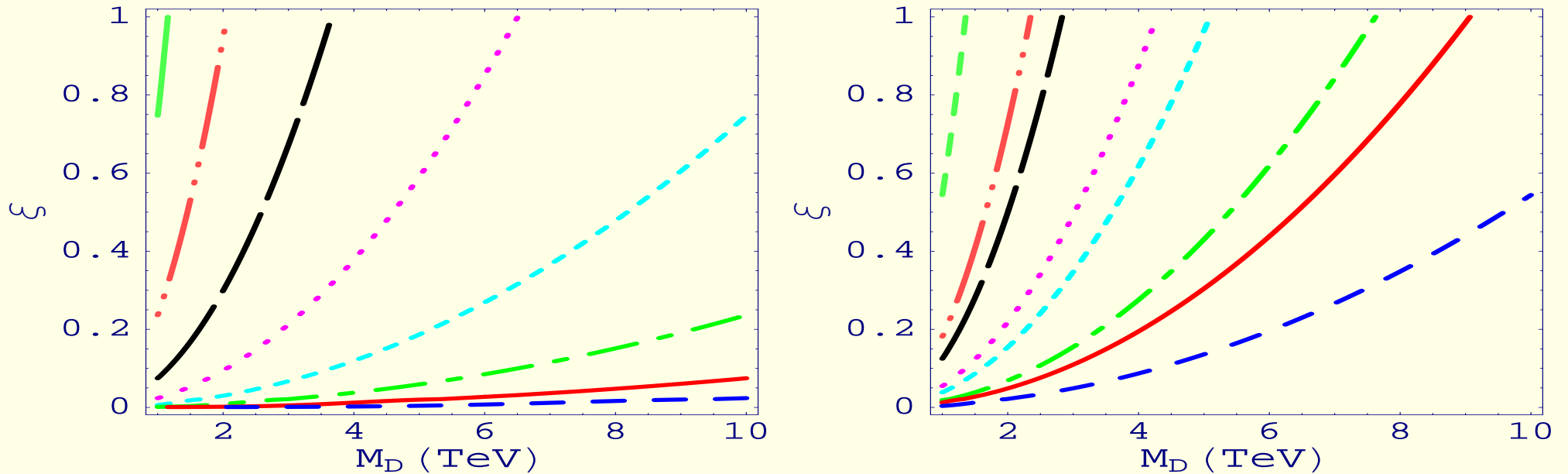


**Figure 5:**  $m_h = 1000$  GeV and  $\delta = 2$ .

Plots for  $m_h = 1000$  GeV and  $\delta = 2$  appear in Fig. 5. Note that in this case,  $\Gamma_h^{SM} \sim 530$  GeV. However, there is a compensating increase with  $m_h$  of the invisible width and so the branching ratio results are not so different from those for  $m_h = 237$  GeV,  $\delta = 2$ .

## Prospects for Discovery at the LHC and a future LC

- For a Higgs boson with  $m_h$  below the  $WW$  threshold, the invisible width causes a significant suppression of the LHC Higgs rate in the standard visible channels.

For example, for  $\delta = 2$ ,  $M_D = 500$  GeV and  $m_h = 120$  GeV,  $\Gamma_{h' \rightarrow \text{graviscalar}}$  is of order 50 GeV already by  $\xi \sim 1$ , *i.e.* far larger than the SM prediction of 3.6 MeV.

Even when  $m_h > 2m_W$ , the branching ratio into invisible states can be substantial for  $M_D$  values as large as several TeV

Therefore, for any given value of the Higgs boson mass, there is a considerable parameter space where the invisible decay width of the Higgs boson could be the first measured phenomenological effect from extra dimensions.

- Production through  $WW$  fusion of the  $h'$  and the  $s'_{\vec{n}}$  states nearly degenerate with it gives an effective "Higgs" production cross section that is equal to the SM  $h$  cross section for any given production mode (*i.e.*, any initial state,  $I$ ).

To determine the rate in any given channel (specified by an initial state  $I$  and final state  $F$ ) of  $h_{eff} \equiv h' + \sum_{\vec{n}>0} s'_{\vec{n}}$  production, we need only take the SM production rate for initial state  $I$  and multiply by the effective branching ratio for  $h_{eff} \rightarrow F$ . We found that

$$BR(h_{eff} \rightarrow invisible) = \frac{\Gamma_{h_{eff} \rightarrow graviscalars}}{\Gamma_h^{SM} + \Gamma_{h_{eff} \rightarrow graviscalars}}, \quad (9)$$

and that the corresponding rates in the usual SM  $h$  decay channels are reduced by  $1 - BR(h_{eff})$ .

- **Visible Channels**

Detailed studies of the Higgs boson signal significance, with inclusive production, have been carried out by the ATLAS [4, 5] and CMS [6] experiments.

We will employ the results of [6]. These were obtained for  $L = 30\text{fb}^{-1}$ . For  $L = 100\text{fb}^{-1}$ , we will simply rescale the statistical significances in each channel by  $\sqrt{100/30}$ .

- **Invisible Channel**

The LHC experiments will also be sensitive to an invisibly decaying Higgs

boson produced via  $WW$ -fusion, as summarized in Ref. [6].

With only  $10 \text{ fb}^{-1}$ , a Higgs boson produced with the SM  $WW \rightarrow \text{Higgs}$  rate and decaying to an invisible final state with  $BR(h \rightarrow \text{invisible}) = 0.12 - 0.28$  exceeds the 95% CL for  $120 \text{ GeV} < m_h < 400 \text{ GeV}$ .

We convert these 95% CL limits to the requirements for  $5\sigma$  discovery and adjust for different luminosities by assuming scaling according to  $\sqrt{L(\text{fb}^{-1})/10}$ .

In this way, we can determine the portion of the  $(M_D, \xi)$  parameter space where the  $h_{eff}$  Higgs signal can be recovered at the  $5\sigma$  level through invisible decays.

- $jets/\gamma + \cancel{E}_T$  at the LHC**

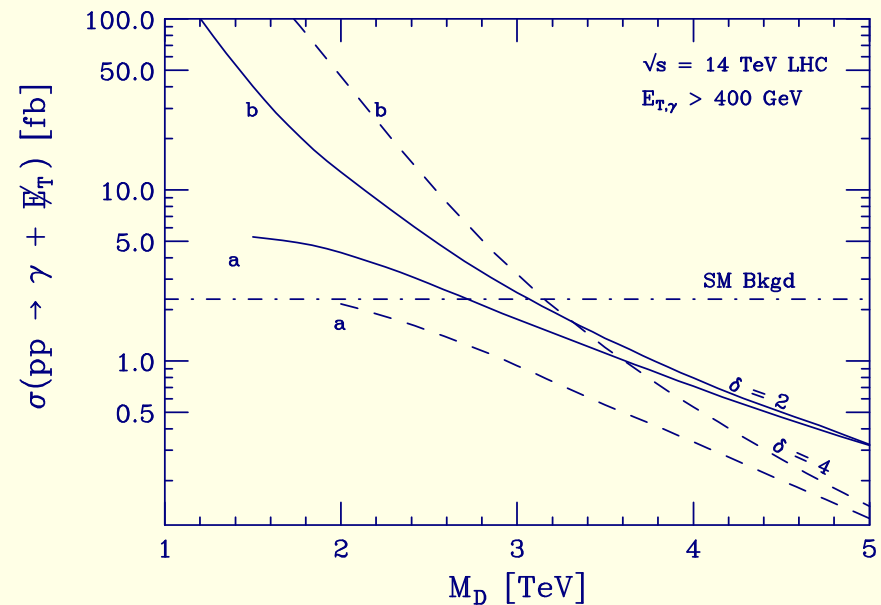
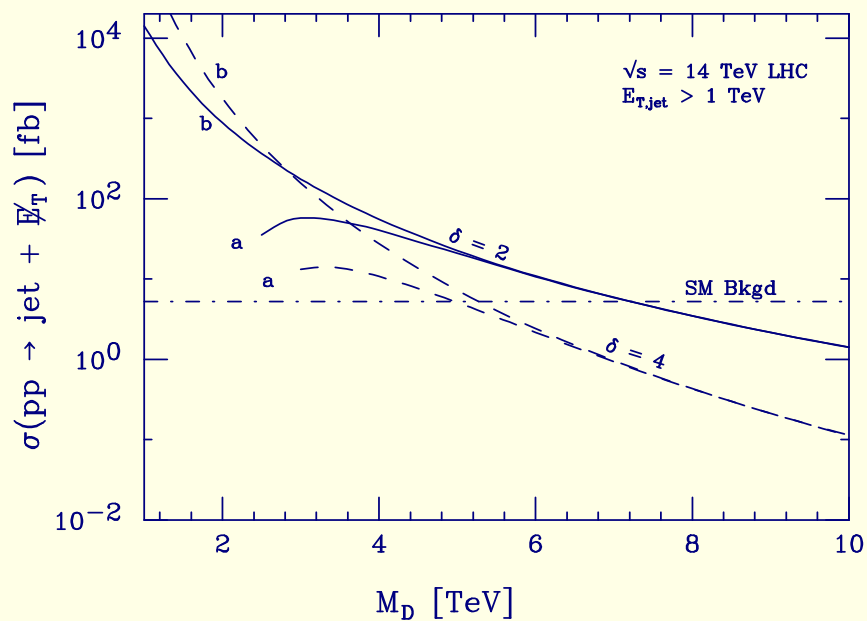


**Figure 6:**  $jets + \cancel{E}_T$  and  $\gamma + \cancel{E}_T$  cross sections after integrating over a)  $\hat{s} < M_D^2$  or b) all  $\hat{s}$ , where  $\hat{s}$  is subprocess  $s$ .

The above figure shows that the prediction of the ADD model for  $jets/\gamma +$

$\mathcal{E}_T$  is only reliable in a very limited range of  $M_D$ .

A signal at low  $M_D$  might or might not be present depending upon how the theoretical result behaves at subprocess energies above  $M_D$ , a region where the theory is not reliable.

Even more importantly, given an observed signal we cannot be sure how to interpret it. **This makes parameter determination via this means at the LHC impossible.**

- LC searches for invisible Higgs decays

A TeV-class  $e^+e^-$  linear collider will be able to see the  $h_{eff}$  Higgs signal regardless of the magnitude of the invisible branching ratio simply by looking for a peak in the  $M_X$  mass spectrum in  $e^+e^- \rightarrow ZX$  events.

As shown in [7], a substantial signal for events in which  $X$  is an invisible final state is possible down to fairly low values of  $BR(h_{eff} \rightarrow invisible)$ .

We have employed the  $\sqrt{s} = 350$  GeV,  $L = 500\text{fb}^{-1}$  results of [7] to determine the portion of  $(M_D, \xi)$  parameter space for which the invisible Higgs signal will be observable at the LC at the  $5\sigma$  or better level.

Not surprisingly, the LC will be able to detect this signal over an even larger part of the parameter space than can the LHC.

- $\gamma + \cancel{E}_T$  at the LC unlike LHC, subprocess energy fixed  $=\sqrt{s}$ .

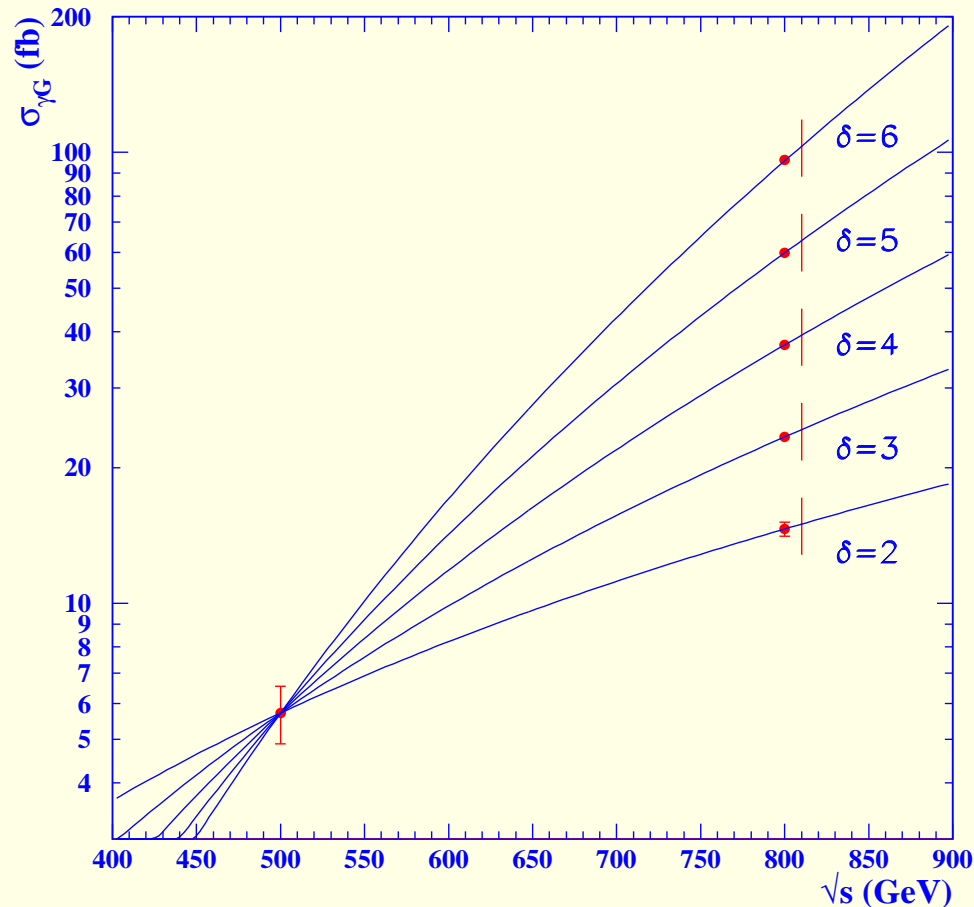


Figure 7:  $\gamma + \cancel{E}_T$  cross sections vs.  $\sqrt{s}$ , normalized to common value at  $\sqrt{s} = 500$  GeV. Thus, energy dependence gives  $\delta$  via ratio of cross sections. Absolute normalization then gives  $M_D$ .

In the following figures (which assume  $L = 100\text{fb}^{-1}$  at LHC):

- Green region = visible channels  $< 5\sigma$  at LHC.
- The regions above the blue line = LHC invisible Higgs signal in the  $WW$ -fusion channel exceeds  $5\sigma$ .
- The solid vertical line = maximum  $M_D$  which can be probed at the  $5\sigma$  level by the analysis of  $jets/\gamma$  with missing energy at the LHC.
- The middle dotted vertical line =  $M_D$  below which the theoretical computation at the LHC is ambiguous — a signal could still be present there, but its magnitude is uncertain.

(For  $\delta = 5$ , there is no value of  $M_D$  for which the LHC computation is reliable.)

- The dashed vertical line at the lowest  $M_D$  value is the 95% CL lower limit coming from combining Tevatron and LEP/LEP2 limits.
- Region above the yellow line = LC invisible Higgs signal exceeds  $5\sigma$  assuming  $\sqrt{s} = 350\text{ GeV}$  and  $L = 500\text{fb}^{-1}$ .

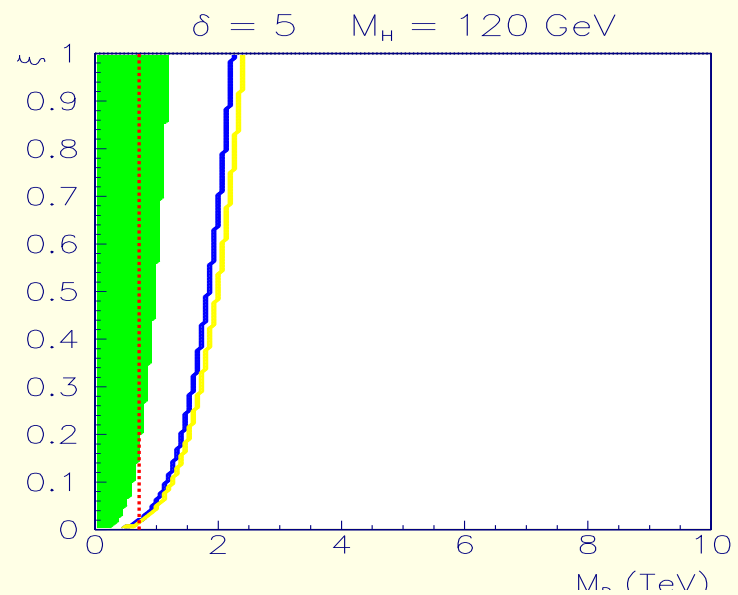
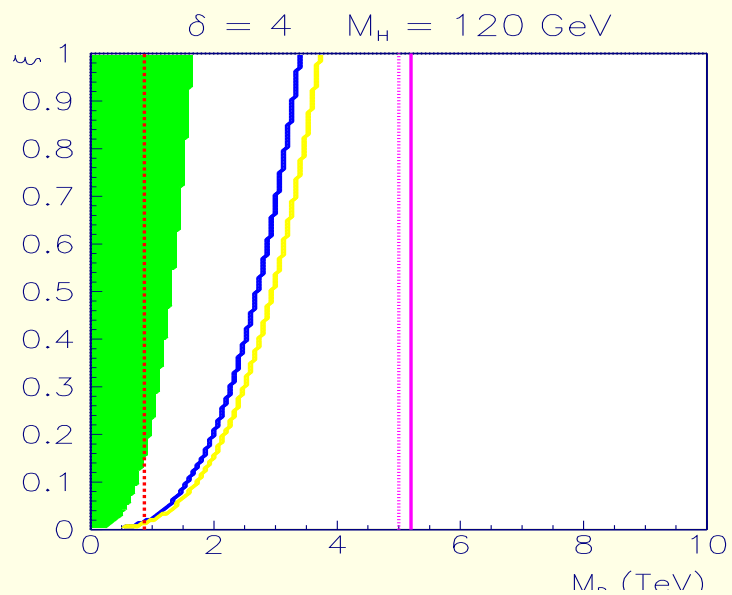
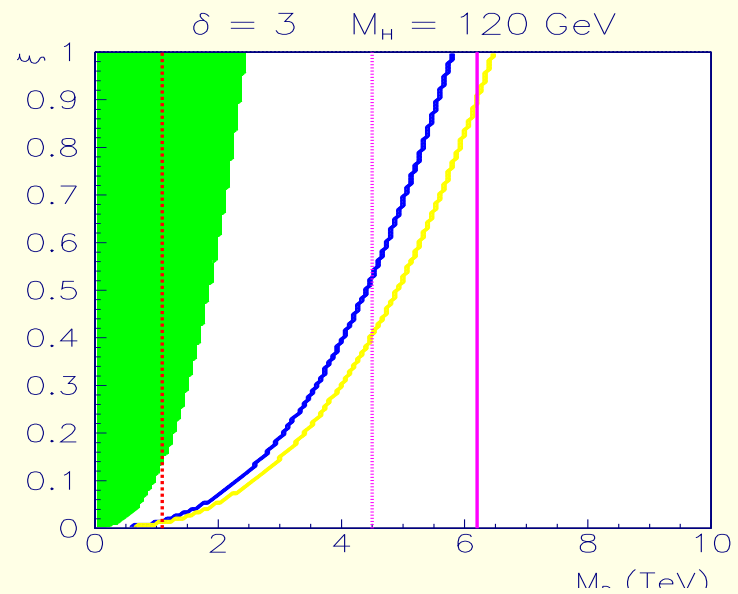
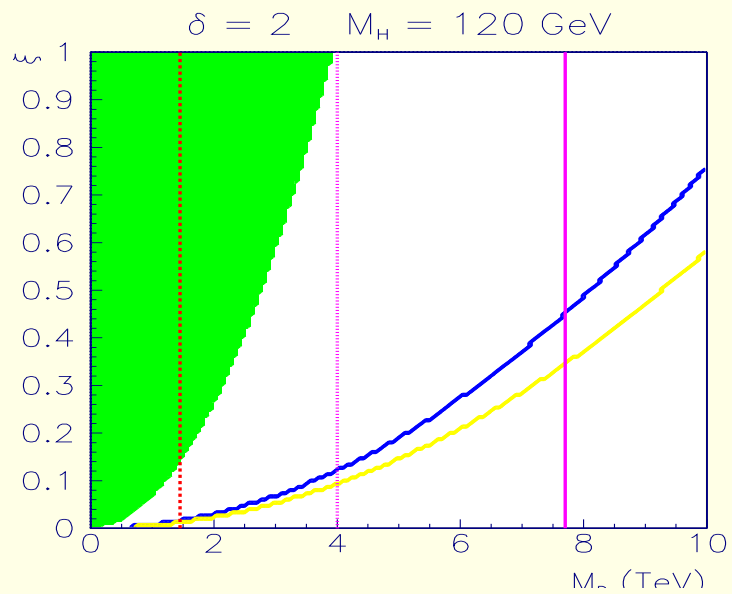


**Figure 8: Results for  $m_h = 120$ .**

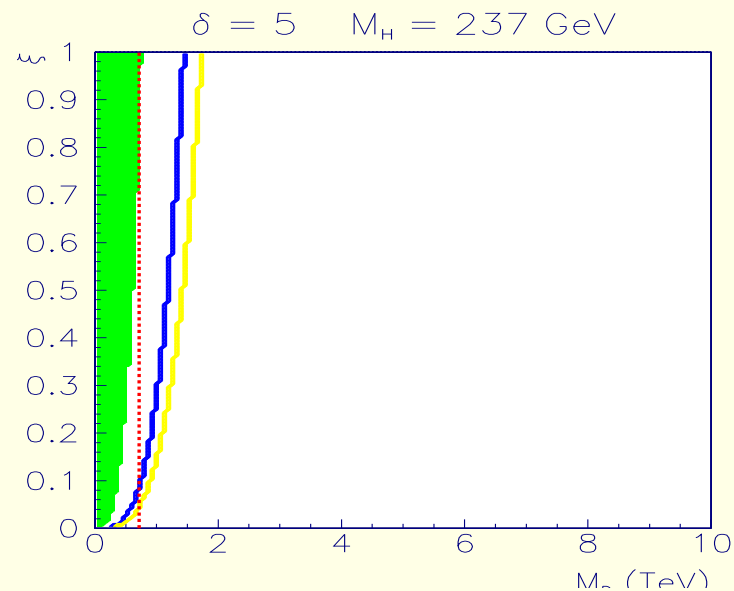
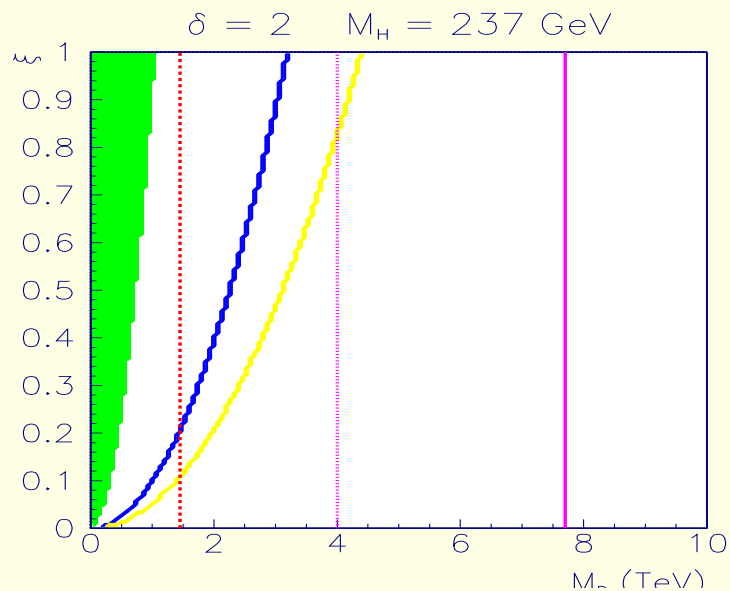


Figure 9: As in Fig. 8, for  $m_h = 237$  GeV and  $\delta = 2$  and  $\delta = 5$ .

- Summary**

Whenever the LHC Higgs boson sensitivity in standard visible decays is lost due to their suppression, the invisible rate is large enough to still ensure detection through a dedicated analysis.

For  $m_h = 237$  GeV, Fig. 9 shows that regions where visible signal  $< 5\sigma$  appear to be fully excluded by LEP and Tevatron.

## Determining ADD parameters from LHC and LC data

- If the LC is operating, the very first test of the model will be to determine if the  $e^+e^- \rightarrow ZX$  events do indeed exhibit a resonance structure with the predicted rate for a SM Higgs with the observed peak mass.

This can be done at about the 3% level.

If this test works, then one can proceed with the parameter determination.

- If the LC is not operating, there will be no decay-mode-independent means for checking that the Higgs is produced with SM-like rate.

At the LHC, this can only be done by looking for consistency of the collection of visible and invisible final state rates in various production modes with the assumption of a SM *production* rate combined with the ADD prediction that the standard visible final state *BR*'s are reduced in rate by the uniform factor of  $1 - BR(h_{eff} \rightarrow invisible)$ .

- We will determine the error with which the LHC can determine the parameters under the assumption that the production cross section for the

Higgs signal in each of the many production modes studied by ATLAS and CMS is SM-like.

The errors on the parameter determinations will be somewhat increased if we allow for the possibility of non-SM production rates. Thus, the results presented for LHC operation alone are somewhat optimistic.

- Our LHC procedures are as follows.
  - For the LHC, we have not made use of the jets/ $\gamma$  +  $\cancel{E}_T$  signal for determining  $M_D$  and  $\delta$  because of theoretical uncertainties described earlier.
  - For the LHC Higgs signal in visible channels, we compute the  $\Delta\chi^2$  for a model relative to expectations as

$$\Delta\chi^2 = \frac{(S - S_0)^2}{\Delta S_0^2} \quad (10)$$

where  $\Delta S_0^2 = S_0 + B$  and  $S$  and  $S_0$  are computed from the SM rates by multiplying by  $1 - BR_{h_{eff} \rightarrow invisible}$  and  $1 - BR_{h_{eff}^0 \rightarrow invisible}$ .

Analogous procedures for  $\Delta\chi^2$  contributions are followed in other channels.

- For the LHC Higgs signal in the invisible final state, we employed the detailed results of [8] (used in [6]), in which the Higgs signal and background event rates are given for the  $WW \rightarrow Higgs \rightarrow invisible$  channel assuming SM production rate and 100% invisible branching ratio.
- A TeV-class  $e^+e^-$  linear collider will be able to improve the determination of the ADD model parameters very considerably with respect to the LHC alone. Here, we make use of the Higgs signals in both visible and invisible final states and also of the  $\gamma + \cancel{E}_T$  signal.
  - For the  $\gamma + \cancel{E}_T$  signal, we have employed the TESLA study results of [9] for the signal.
 

We will present results obtained assuming measurements performed at the two energies of  $\sqrt{s} = 500$  GeV and  $\sqrt{s} = 1000$  GeV assuming integrated luminosities of either  $500\text{fb}^{-1}$  and  $1000\text{fb}^{-1}$ , respectively, or  $1000\text{fb}^{-1}$  and  $2000\text{fb}^{-1}$ , respectively.

The reason for considering two energies is that the ratio of the cross sections at the two energies gives a strong constraint on  $\delta$ , independent of cross section normalization. The value of  $M_D$  can then be thought of as being determined by the absolute value of the cross sections.
  - For the invisible Higgs signal, we employ the  $\sqrt{s} = 350$  GeV results of [7].

– For the visible Higgs signal, we employ a simple summary of the best available LC errors on the various SM Higgs signals, especially the  $b\bar{b}$  and  $WW^{(*)}$  final states, assuming running at energies of  $\sqrt{s} = 500$  GeV and  $\sqrt{s} = 1000$  GeV with luminosities of at least  $500\text{fb}^{-1}$  and  $1000\text{fb}^{-1}$ , respectively, and with polarization.

We do not consider  $m_h > 500$  GeV.

- The  $BR_{h_{eff} \rightarrow \text{visible}}$  measurement turns out to be quite important in discriminating between different models when the invisible branching fraction is large (the latter requiring small to moderate  $m_h$ , small  $M_D$ ,  $\delta = 2$  or  $3$ , depending on  $M_D$ , and substantial  $\xi$ ).

In such a case, the visible branching fraction can be quite small and typically varies rapidly as a function of the ADD parameters (in particular,  $\xi$ ), whereas the invisible branching fraction, although large, will be relatively more slowly varying and will not provide as good a discrimination between different parameter choices.

Of course, if  $BR_{h_{eff} \rightarrow \text{visible}}$  is so small that the background is dominant, the error in the measurement deteriorates and our ability to determine  $\xi$ ,  $M_D$  and  $\delta$  from this measurement deteriorates.

- Complementary statements apply to the case when  $BR_{heff \rightarrow invisible}$  is small and  $BR_{heff \rightarrow visible}$  is slowly varying.

In particular, the right-hand plot of Fig. 1 shows that  $BR_{heff \rightarrow invisible}$  varies very rapidly with  $\xi$  at small  $\xi$  in the case of  $m_h = 120$  GeV,  $\delta = 2$ , even for quite large  $M_D$ .

As  $\delta$  increases, the branching ratio contours become more vertical, as illustrated in the  $\delta = 4$  right-hand plot of Fig. 2, and it becomes more difficult to determine  $\xi$  accurately.

- In the best cases, the visible and invisible branching fractions are comparable and both are rapidly varying as a function of  $\xi$  and the other ADD parameters. In such a case, measurements of these branching fractions combine to yield an excellent determination of all the ADD parameters.
- Given the (currently) five different  $\Delta\chi^2$  outlined above, which we denote by  $\Delta\chi^2(LHC Hvis)$ ,  $\Delta\chi^2(LHC Hinv)$ ,  $\Delta\chi^2(LC \gamma\cancel{E}_T)$ ,  $\Delta\chi^2(LC Hinv)$ , and  $\Delta\chi^2(LC Hvis)$ , respectively, the net discrimination between models can be characterized using

$$\Delta\chi^2(LHC) = \Delta\chi^2(LHC Hvis) + \Delta\chi^2(LHC Hinv)$$

$$\Delta\chi^2(LC) = \Delta\chi^2(LC \gamma\cancel{E}_T) + \Delta\chi^2(LC Hinv) + \Delta\chi^2(LC Hvis)$$

$$\Delta\chi^2(LHC + LC) = \Delta\chi^2(LHC) + \Delta\chi^2(LC). \quad (11)$$

- Since we assume that  $m_h$  will be very precisely measured, we concentrate on our ability to determine the parameters  $M_D$ ,  $\delta$  and  $\xi$ .

We will present regions of parameter space corresponding to 95% CL determination, which for three parameters corresponds to  $\Delta\chi^2 = 7.82$ .

Some sample results appear in Figs. 10–13, where we continue to focus on the light Higgs mass case of  $m_h = 120$  GeV and the heavier Higgs case of  $m_h = 237$  GeV.

- In the first figure, we present 95% CL contours for determination of the ADD parameters,  $M_D$ ,  $\xi$  and  $\delta$  assuming  $m_{h_{eff}} = 120$  GeV. The plots are all for input values if  $\delta^0 = 2$  and  $\xi^0 = 0.5$ .

The upper two plots and lower left plot are obtained assuming  $L = 100\text{fb}^{-1}$  at the LHC,  $\sqrt{s} = 350$  GeV Higgs measurements at the LC, and  $\sqrt{s} = 500$  GeV and  $\sqrt{s} = 1000$  GeV  $\gamma + \cancel{E}_T$  measurements at the LC with  $L = 1000\text{fb}^{-1}$  and  $L = 2000\text{fb}^{-1}$  at the two respective energies. They

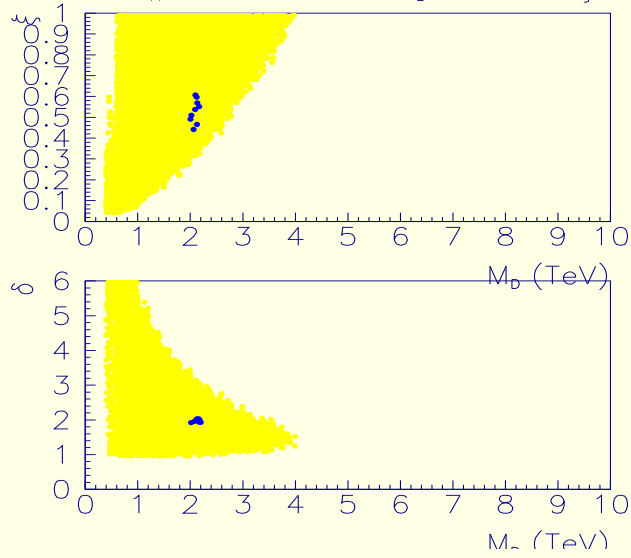
are for different  $M_D^0$  values: upper left —  $M_D^0 = 2$  TeV; upper right —  $M_D^0 = 5$  TeV; lower left —  $M_D^0 = 8$  TeV.

The lower right plot is a repeat of the  $M_D^0 = 5$  TeV case, but assuming lower integrated luminosities:  $L = 30\text{fb}^{-1}$  at the LHC and  $L = 500\text{fb}^{-1}$  and  $L = 1000\text{fb}^{-1}$  at  $\sqrt{s} = 500$  GeV and  $\sqrt{s} = 1000$  GeV at the LC.

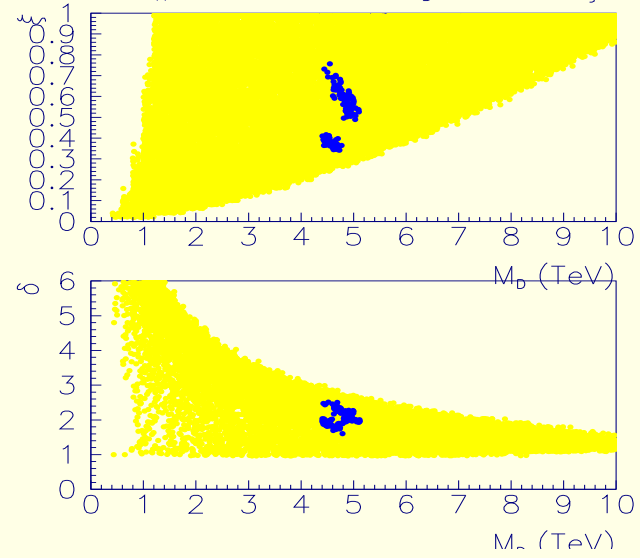
The larger light grey (yellow) regions are the 95% CL regions in the  $\xi, M_D$  and  $\delta, M_D$  planes using only  $\Delta\chi^2(LHC)$ .

The smaller dark grey (blue) regions or points are the 95% CL regions in the  $\xi, M_D$  and  $\delta, M_D$  planes using  $\Delta\chi^2(LHC + LC)$ .

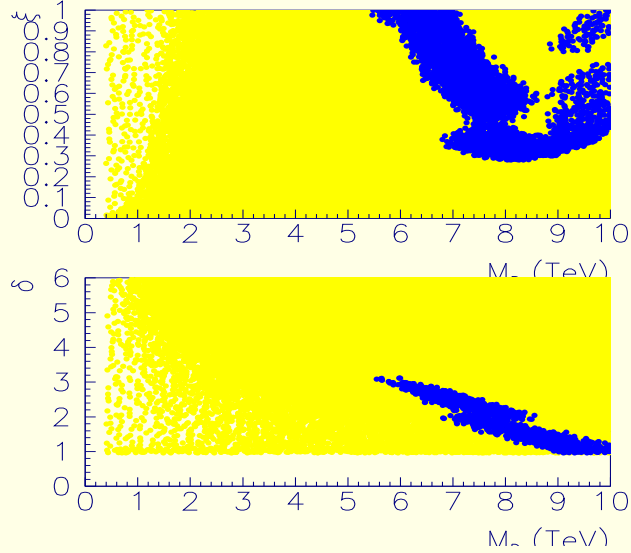
$\delta = 2, M_H = 120 \text{ GeV}, M_D = 2 \text{ TeV}, \xi = .5$



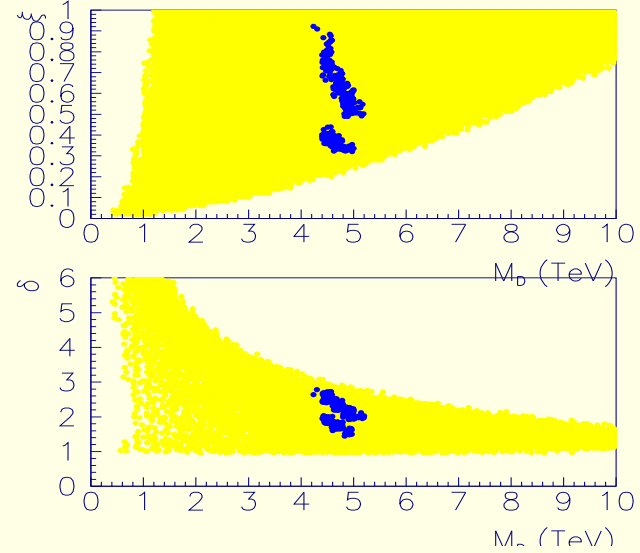
$\delta = 2, M_H = 120 \text{ GeV}, M_D = 5 \text{ TeV}, \xi = .5$



$\delta = 2, M_H = 120 \text{ GeV}, M_D = 8 \text{ TeV}, \xi = .5$



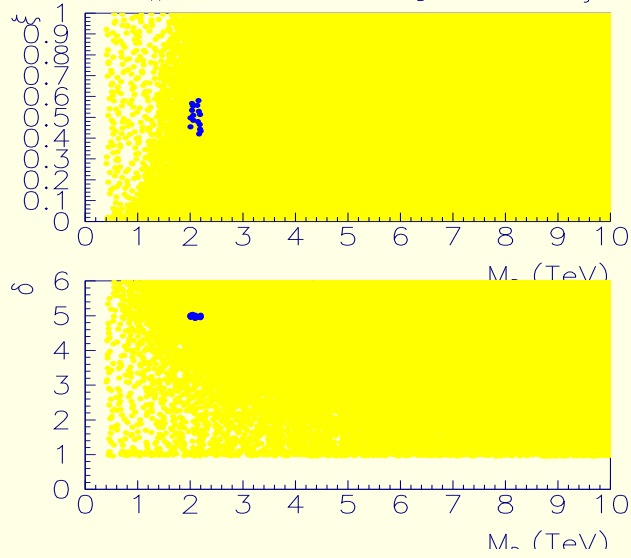
$\delta = 2, M_H = 120 \text{ GeV}, M_D = 5 \text{ TeV}, \xi = .5$



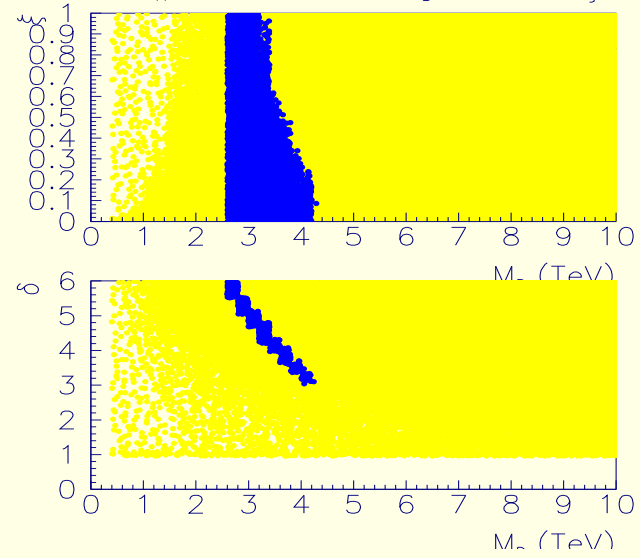
**Figure 10:**

Figure 11 considers the higher  $\delta$  values of 4 and 5. The first three subfigures show again the decrease of precision with increasing  $M_D$ . (Adequate precision is lost at a lower  $M_D$  value than for  $\delta = 2$ .) Comparing the lower right to lower left figure, we see that at fixed  $M_D$  and  $\xi$  the precision of parameter determination increases as  $\delta$  is lowered.

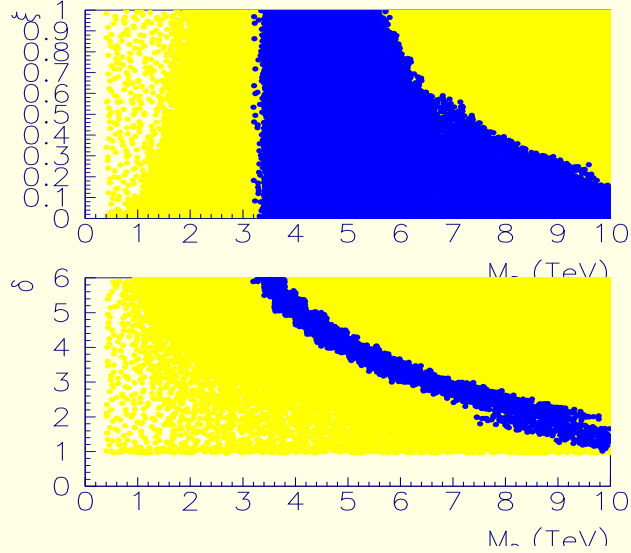
$\delta = 5, M_H = 120 \text{ GeV}, M_D = 2 \text{ TeV}, \xi = .5$



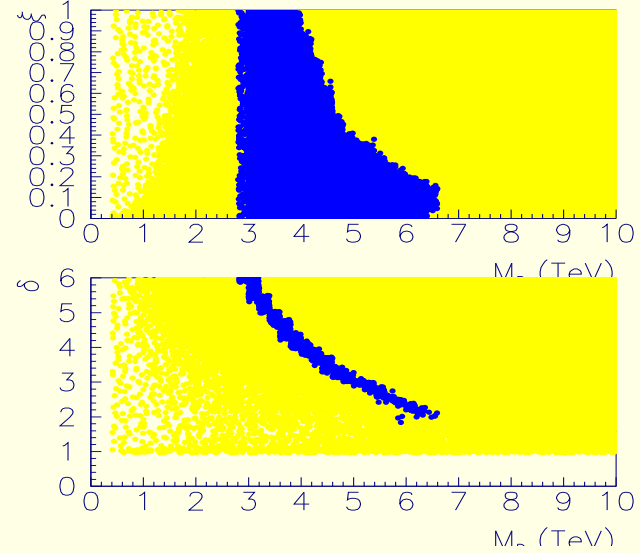
$\delta = 5, M_H = 120 \text{ GeV}, M_D = 3 \text{ TeV}, \xi = .5$



$\delta = 5, M_H = 120 \text{ GeV}, M_D = 4 \text{ TeV}, \xi = .5$



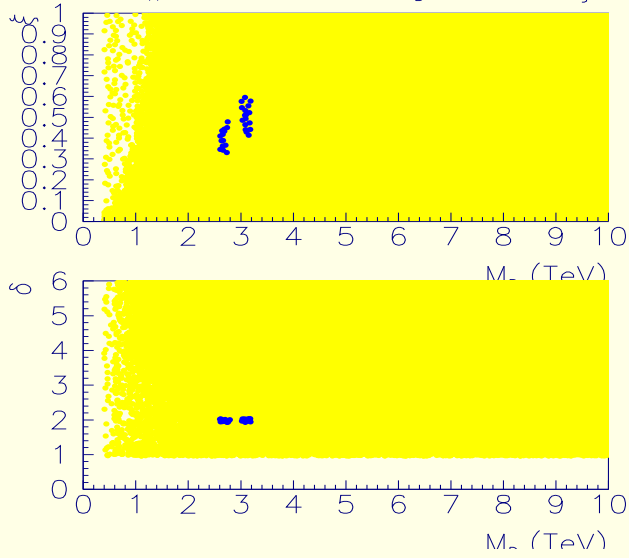
$\delta = 4, M_H = 120 \text{ GeV}, M_D = 4 \text{ TeV}, \xi = .5$



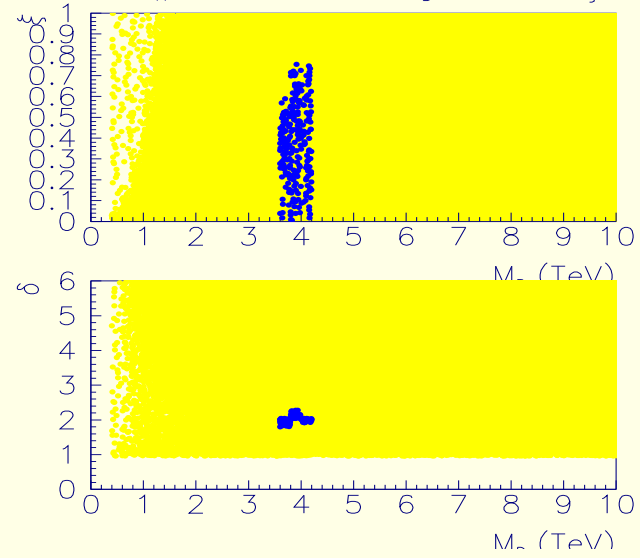
**Figure 11:**

Figure 12 considers  $m_h = 237$  GeV for a selection of  $M_D$ ,  $\xi$  and  $\delta$  input values. We see that for  $\xi = 0.5$  a good determination of  $\xi$  is only possible if both  $M_D$  and  $\delta$  are not large. The larger  $\xi$  is, the larger the  $M_D$  and  $\delta$  values for which  $\xi$  determination would be possible.

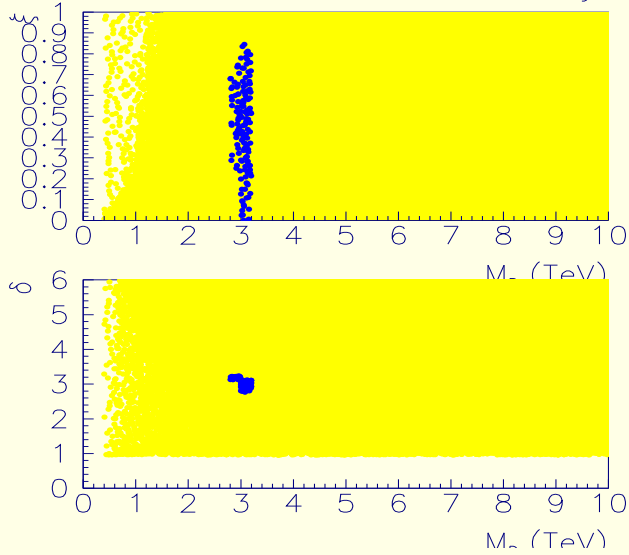
$\delta = 2, M_H = 237 \text{ GeV}, M_D = 3 \text{ TeV}, \xi = .5$



$\delta = 2, M_H = 237 \text{ GeV}, M_D = 4 \text{ TeV}, \xi = .5$



$\delta = 3, M_H = 237 \text{ GeV}, M_D = 3 \text{ TeV}, \xi = .5$



$\delta = 4, M_H = 237 \text{ GeV}, M_D = 3 \text{ TeV}, \xi = .5$

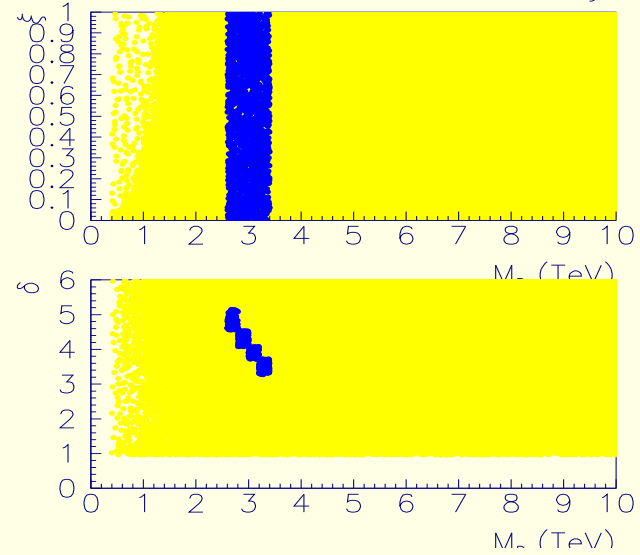


**Figure 12:**

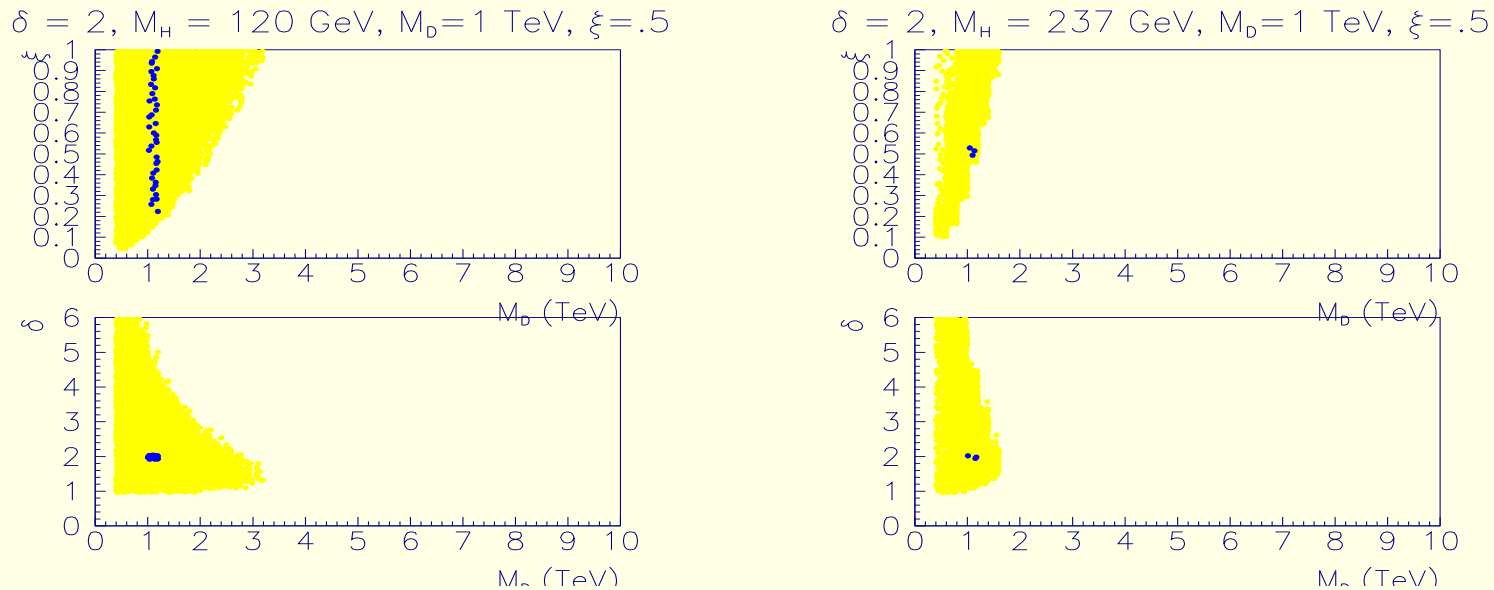


**Figure 13:**

Finally, in Fig. 13, we show some results for the low value of  $M_D = 1$  TeV. We also take  $\delta = 2$  and  $\xi = 0.5$ . These choices result in substantial invisible decays. In the plots, we consider  $m_h = 120$  GeV and  $m_h = 237$  GeV.

In the  $m_h = 120$  GeV case,  $\xi$  is not well determined. This is because the error on the SM visible decay modes is large in this case (because of very small branching ratio,  $BR_{h_{eff} \rightarrow visible} \lesssim 1\%$ , the background is much bigger than the signal) while the invisible decay branching fraction is very slowly varying as a function of the parameter  $\xi$ .

This is to be contrasted with the  $m_h = 237$  GeV case, where we see that the determination of  $\xi$  is excellent. This is a case in which

the visible and invisible branching ratios are comparable ( $BR_{h_{eff} \rightarrow visible} = 1 - BR_{h_{eff} \rightarrow invisible} \sim 0.35$ ), have very small errors ( $E_{vis} \sim 0.016$ ,  $E_{inv} \sim 0.021$ ), and are rapidly varying as a function of  $\xi$ .

## Conclusions

- If the Higgs boson is light (we have focused on  $m_h = 120$  GeV and the current 95% CL upper limit from precision electroweak data of 237 GeV), then the invisible final state Higgs signal at the LHC could provide the most definitive evidence for the existence of extra dimensions before LC operation unless the mixing parameter  $\xi$  is much smaller than its expected  $\mathcal{O}(1)$  magnitude.
- However, although the LHC has a good chance of seeing a signal, it will not be able to determine  $M_D$ ,  $\delta$  and  $\xi$  with any real precision.

In particular,  $jets/\gamma + \cancel{E}_T$  predictions as a function of  $M_D$  and  $\delta$  are ambiguous in such a way that a given signal rate cannot be reliably interpreted.

- A variety of measurements at the LC will be required:
  - $\gamma + \cancel{E}_T$ ,
  - Higgs production/decay in the usual visible SM-like final states,
  - and Higgs production/decay in the invisible final state.

Once these measurement have been made with the high precision expected at the LC, the  $M_D$ ,  $\delta$  and  $\xi$  will be determined with good to reasonable accuracy so long as not both  $\delta$  and  $M_D$  are large.